



Deep kinematic inference affords efficient and scalable control of bodily movements

Matteo Priorelli^a, Giovanni Pezzulo^b, and Ivilin Peev Stoianov^{a,1}

Edited by Peter Strick, University of Pittsburgh Brain Institute, Pittsburgh, PA; received May 31, 2023; accepted October 24, 2023

Performing goal-directed movements requires mapping goals from extrinsic (workspace-relative) to intrinsic (body-relative) coordinates and then to motor signals. Mainstream approaches based on optimal control realize the mappings by minimizing cost functions, which is computationally demanding. Instead, active inference uses generative models to produce sensory predictions, which allows a cheaper inversion to the motor signals. However, devising generative models to control complex kinematic chains like the human body is challenging. We introduce an active inference architecture that affords a simple but effective mapping from extrinsic to intrinsic coordinates via inference and easily scales up to drive complex kinematic chains. Rich goals can be specified in both intrinsic and extrinsic coordinates using attractive or repulsive forces. The proposed model reproduces sophisticated bodily movements and paves the way for computationally efficient and biologically plausible control of actuated systems.

motor control | kinematics | neurocomputational modeling | predictive coding | active inference

How do the brains of living systems support goal-directed movements implementing purposeful behavior? A standard assumption is that performing goal-directed actions requires two mappings reflecting perceptual and plant control processes (1). First, it is necessary to map goals and desired movement trajectories specified in extrinsic coordinates (e.g., in Cartesian space) into movements specified in intrinsic coordinates (e.g., as joint angles), via a process called inverse kinematics. Second, it is necessary to map the intrinsic state into the forces needed to move all the muscles of the body, via a process called inverse dynamics.

These two inversions (kinematic and dynamic) are computationally challenging. While computing the extrinsic representation of a given joint configuration is easy as the geometric mapping—the so-called direct kinematics—is univocal, finding the joint angles that correspond to a particular position is not straightforward. Computing a motor plan that brings the agent to that posture is even more difficult, since there are multiple possibilities of how the movement may be realized—and the computational complexity increases with the Degrees of Freedom (DoF) of the kinematic chain (e.g., a single arm versus the entire body).

Mainstream theories based on optimal control provide a solution to the two inversions that rests upon the optimization of a cost function (2–6). However, realizing certain movements such as handwriting or walking is difficult, since not all trajectories have well-defined cost functions (7). Furthermore, the required computations are usually demanding as the model inversion requires considering the effects of the executed actions. Because the latter are perceived with delays that vary across and within sensory modalities (8, 9), they need to be compensated using a forward model, which could introduce additional errors (10).

Active inference offers an alternative scheme that does not require cost functions (7, 11–15). It proposes that agents are endowed with a generative model specifying the dynamics of their hidden states (e.g., hand positions over time) and that desired goals are encoded as priors over the dynamics (e.g., desired hand positions), which act as attracting states (16). Goal-directed movements are realized by first generating proprioceptive predictions from the hidden states and then minimizing proprioceptive prediction errors, or the discrepancy between predicted and current sensations. Crucially, the mapping between proprioceptive predictions and control signals for the muscles is quite simple and can be implemented with minimal latency using reflex arcs in the spinal cord rather than requiring complex inverse dynamics computations (13). In fact, the inverse model maps from proprioceptive sensations to actions, not from hidden states (either in intrinsic or extrinsic coordinates) to actions, as in optimal control (10).

Note that active inference only uses reflex arcs as the last stage of control. Complex motor patterns are not constructed at the level of reflex arcs, but rather generated by high-level dynamics that predict specific patterns of proprioceptive predictions (17).

Significance

How can we realize sophisticated purposeful movements? While agile motor control is now standard in robotics, the computational machinery supporting this capacity in biological organisms remains controversial. Active inference theory assumes that actions arise by inferring limb trajectories from the desired effects in an exteroceptive (e.g., visual) space. Yet, how it enables efficient motor control is unclear. Our innovative solution rests on designing a hierarchical kinematic model that mimics the body structure and predicts the exteroceptive effects of movements. Tasks like drawing a circle, reaching and avoiding objects are realized efficiently because the transformation of the desired movements from the exteroceptive domain into limb trajectories are computed as deep inference in the model, using biologically plausible local computations only.

Author affiliations: ^aNational Research Council, Institute of Cognitive Sciences and Technologies, Padova 35137, Italy; and ^bNational Research Council, Institute of Cognitive Sciences and Technologies, Rome 00185, Italy

Author contributions: M.P. and I.P.S. designed research; G.P. contributed further to the design; M.P. performed research; M.P. contributed new reagents/analytic tools; M.P. analyzed data; and M.P., G.P., and I.P.S. wrote the paper.

The authors declare no competing interest.

This article is a PNAS Direct Submission.

Copyright © 2023 the Author(s). Published by PNAS. This article is distributed under Creative Commons Attribution-NonCommercial-NoDerivatives License 4.0 (CC BY-NC-ND).

¹To whom correspondence may be addressed. Email: ivilinpeev.stoianov@cnr.it.

This article contains supporting information online at <https://www.pnas.org/lookup/suppl/doi:10.1073/pnas.2309058120/-DCSupplemental>.

Published December 12, 2023.

Such predictions encode not just positional terms, but also higher temporal orders (18), allowing the reflex arcs to realize sophisticated instantaneous trajectories that comprise, e.g., velocities and torques (19, 20). Furthermore, prior expectations over the model dynamics and the entire hierarchy allow immediate first-guess responses, which are eventually refined by subsequent feedback (1).

While there is increasing interest in using active inference methods for biological control and robotics (21–29), their application in realistic settings has been limited so far, given two fundamental issues. First, realizing generative models that afford effective kinematic inversions is challenging. State-of-the-art robotic implementations skip the kinematic inversion and realize movements by only relying on intrinsic coordinates (19, 30). Despite their effectiveness, such schemes do not allow specifying goals in extrinsic coordinates and hence have several practical limitations. Other approaches embed conventional optimal control inversions, such as the Jacobian transpose (10, 31) or the pseudoinverse (32) directly within the dynamics of the hidden states. This has the disadvantage that extrinsic and intrinsic coordinates are mixed up and some computations are duplicated: Extrinsic priors are mapped into intrinsic coordinates, which in turn generate the extrinsic predictions to be compared with sensory observations. Hence, the extrinsic generative model has to be embedded also in the dynamics function.

Second, and crucially, the above systems do not model (i.e., maintain probabilistic beliefs about) the entire kinematic chain of the body to be controlled, but only the end effector. Therefore, they fall short of addressing naturalistic bodily movements that require the simultaneous coordination of multiple limbs and joints within a complex kinematic chain—such as the body of living organisms—and they cannot account for movement restrictions due to obstacles.

Here, we introduce an active inference architecture that resolves the two above limitations and achieves effective and scalable motor control. First, we show that a generative model

that maps intrinsic into extrinsic coordinates (IE model) affords an effective kinematic inversion through inference. Second, we show that replicating the scheme of the IE model to mimic the hierarchical structure of the agent's kinematic chain affords scalable control of bodily movements.

Results

Kinematic Inversion through an Intrinsic-Extrinsic Model.

Active inference can afford effective motor control through a kinematic generative model that connects two layers of latent states, encoding intrinsic (μ_i) and extrinsic (μ_e) coordinates, respectively (Fig. 1A). This “Intrinsic–Extrinsic (IE) model” has two appealing features compared to optimal control models and previous active inference implementations.

First, the kinematic inversion—or the mapping from extrinsic to intrinsic coordinates—emerges naturally from inference, by inverting the generative mapping from joint angles to Cartesian positions $\mu_e = g_e(\mu_i)$. This means that the latter does not need to be also specified in the model's dynamics function (10, 31, 32). In short, an extrinsic attractor (e.g., a point to be reached) first drives the inference of the most likely intrinsic hidden state at the level above. Then, the latter affects movement execution through the pathway that generates proprioceptive predictions and finally motor commands.

Second, this scheme allows specifying priors at both intrinsic and extrinsic levels simultaneously, which is needed to realize advanced movements with multiple constraints (e.g., moving the arm while keeping the hand horizontally). Specifying attractors at the intrinsic level is also useful for dealing with particular actions for which this is more natural, or when extrinsic goals are difficult to define. For example, grasping actions can be achieved by specifying priors over object-specific joint configurations (e.g., precision grip for small objects or power grip for large objects).

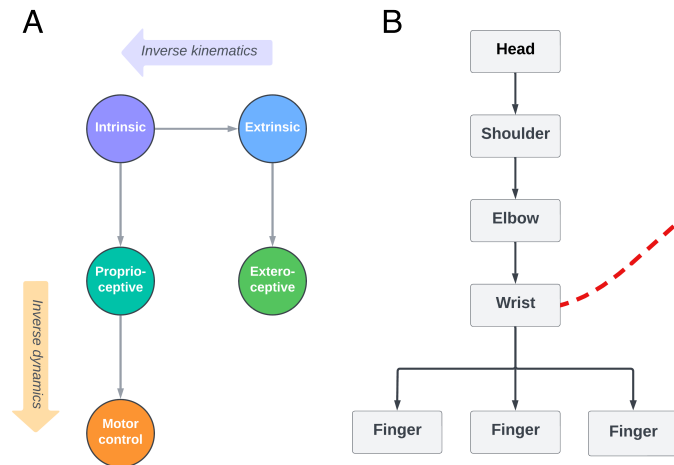
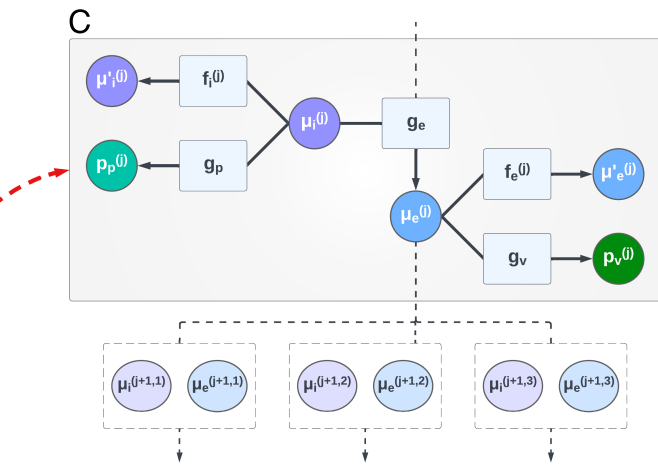


Fig. 1. Generative models for deep kinematic inference. (A) The Intrinsic-Extrinsic (IE) generative model. The two hidden states are intrinsic and extrinsic coordinates, each with its own dynamics. The proprioceptive generative model extracts joint angles from the intrinsic belief, which are used for both posture inference and movement. At the same time, the exteroceptive model produces a visual prediction (in the simulations reported below, it is approximated by directly using the absolute position of the hand). Inverse kinematics is performed by inference, via backpropagation of extrinsic prediction errors. On the other hand, inverse dynamics from proprioceptive predictions to motor control signals is realized through reflex arcs. (B) The deep hierarchical generative model that extends the IE model. The deep model is exemplified for the control of a kinematic plant composed of seven blocks arranged hierarchically, from head to fingers (note that the bottom level is branched, as there are three fingers). Here, the highest (head) level only encodes an extrinsic offset, namely, the initial position and orientation of the origin's reference frame. (C) Factor graph of a single level of the deep hierarchical model. Each block j has the same structure as the kinematic generative model shown in Panel A, but with slight differences. In short, intrinsic beliefs $\mu_i^{(j)}$ and extrinsic beliefs $\mu_e^{(j)}$ are linked by a generative kinematic model g_e , and they encode information about a single kinematic level. They generate proprioceptive predictions $p_p^{(j)}$ and visual predictions $p_v^{(j)}$ only at their specific level. Intrinsic and extrinsic beliefs have their own dynamics, encoded in the functions $f_i^{(j)}$ and $f_e^{(j)}$, which predict future trajectories and are used for goal-directed behavior. Finally, the extrinsic belief at each level j acts as a prior for the level below $j + 1$.

Extending the IE Model to Mimic the Kinematic Chain. The IE model introduced above affords efficient control but still performs the direct kinematics in a single step; in other words, it does not predict the Cartesian coordinates of the entire kinematic chain (e.g., the body), but only the position of the end effector (e.g., the hand). However, the IE model can be extended hierarchically in a straightforward manner, by noting that the direct kinematics of a complex structure can be always decomposed into a sequence of identical transformations (rotations and translations), one for each component of the chain. We exploit this fact to design a hierarchical generative model, composed of as many structurally identical blocks as the number of elements of the kinematic chain where, crucially, each block is an IE model (Fig. 1 *B* and *C*).

This hierarchical architecture affords direct kinematics by iterating the same operation across all the levels of the kinematic chain, with biologically plausible local message passing. Specifically, the Cartesian position of the tip of the body segment at level j is generated from the intrinsic belief over the body segment at the same level and the extrinsic belief over the body segment at the level above $j - 1$. Conversely, the (inverse kinematics) inference of the extrinsic belief at level j requires messages from all the extrinsic beliefs at the level below $j + 1$. In fact, as shown in Fig. 1B, multiple fingers are attached to the same joint at the bottom level (the wrist). The ramifications can be easily treated by assuming that the inference of the hidden states of the block at level j uses the average of the prediction errors generated by all the blocks at the level below $j + 1$ (33). See *Materials and Methods* for more information.

Overall, this biologically plausible form of local message passing is the same as in hierarchical Predictive Coding for perceptual inference (34, 35). Here, top-down and bottom-up

messages across blocks encode kinematic predictions and kinematic prediction errors, respectively.

Defining Goals for Movement using Attractive or Repulsive Forces. In active inference, goals for movements can be either imposed as a higher-level prior or embedded into the dynamics function at the same level. The latter approach is usually based on attractors that linearly minimize the distance between the current and desired states. To generate a dynamic goal, the desired state can also depend on some components of the belief itself through a function that embeds movement intentions (16, 36)—see *Materials and Methods*.

The deep kinematic model introduced here permits formulating various kinds of goals at intrinsic and extrinsic levels; for example, the desired angle θ^* of a joint, the desired absolute position (x^*, y^*) , or orientation ϕ^* of a limb. In addition, it is possible to realize avoidance goals, as shown in *Materials and Methods*. Like attractive forces, repulsive forces are specified for each block of the kinematic chain, which ensures that every segment (rather than just the end effector) is pushed away from an obstacle. Finally, it is possible to define multiple goals simultaneously—such as reaching a particular position with the elbow while maintaining a vertical hand orientation—by combining multiple attractive and/or repulsive forces at different levels. This makes the deep model scalable and versatile, as we show in the next section.

Applications of Deep Kinematic Inference.

Reaching task. We demonstrate the capacity of the deep kinematic model in various motor tasks of increasing complexity. We start from the simple reaching task illustrated in Fig. 2A, which consists of moving a 4R robotic arm (blue) with realistic

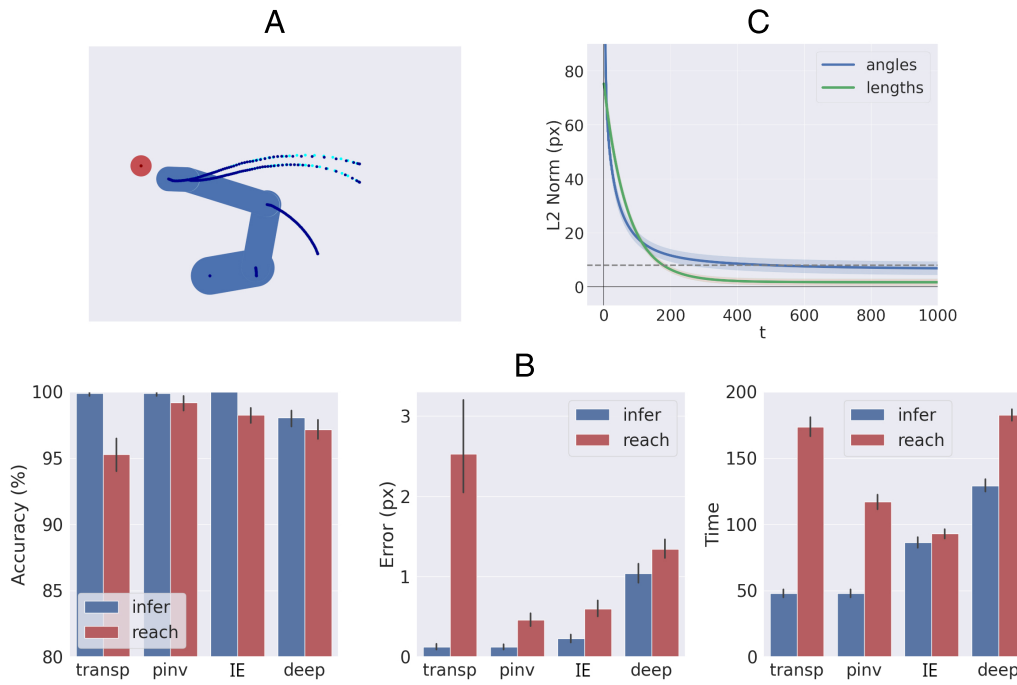


Fig. 2. Results. (A) Simulation setup: a 4R robotic arm with realistic joint limits reaching a static target (red circle). The trajectory of each joint is shown with blue lines. (B) Comparison between the deep kinematic model (deep), the simpler IE model (IE), and two standard active inference controllers based on Jacobian transpose (transp) and pseudoinverse (pinv). The blue and red bars denote the performance of the models during perceptual inference and reaching, respectively. Note that to better probe the model's ability to perform perceptual inference, we only allow the model to use visual observations, but not proprioceptive observations during this phase (however, the model can still use proprioceptive observations for reaching). (C) Evolution over time of the difference between true and estimated end effector positions (blue line), and between true and estimated lengths of the body segments (green line), aggregated over 1,000 trials during inference only. The dashed gray line represents the minimum distance defining a successful inference.

joint limits, to reach a static object (red). Here, we compare the performance of the deep kinematic model (deep) with the simpler IE model (IE) and two alternative controllers based on the Jacobian transpose (transp) and the pseudoinverse (pinv). See *SI Appendix* for more details about the latter two controllers.

The simulation results illustrated in Fig. 2B shows the performance of the four models for 1,000 trials, with 500 steps for trial. For each trial, the beliefs of the models are initialized with random joint angles and segment positions (a more challenging scenario than starting from congruent intrinsic–extrinsic beliefs). Furthermore, a random target location is sampled and set as the reaching goal for the end effector. We evaluate the performance of the four models with regard to both perceptual inference (blue bars) and reaching ability (red bars), using various metrics (see Fig. 2B and *Materials and Methods*).

The performance of the four models is near-optimal during both perceptual inference and reaching. The rare failures are trials in which the models find impossible trajectories and therefore cannot reach the target configurations (note that we did not include any prior over the direction of movement). The performance of the deep model is on par with the other models. The slightly lower performance compared to the IE model is due to the deep model requiring more time to propagate messages across levels, resulting in failed trials when the time steps are limited. The Jacobian pseudoinverse method performs slightly better than the other models, but the transpose method has a much higher final error. Nevertheless, in all cases, the average final error is below the minimum distance to consider a trial successful.

Learning and adaptation of the kinematic chain. Unlike state-of-the-art implementations, the deep model includes beliefs about the length of the body segments and can infer them over time, based on sensory observations. This may afford the rapid adaptation of the agent to changes in the kinematic chain, e.g., when using a tool that increases the length of the last segment, or when a new joint is added to a specific position. To assess this capability, we performed an experiment in which the beliefs about both angles and body segments are randomly initialized. We evaluated the task over 1,000 trials, by comparing the estimated positions of every segment (computed from the joint angles

belief) and the estimated lengths with the real values of the same variables. The simulation results illustrated in Fig. 2C show that the deep model successfully infers the length of its body segments (green line) in addition to inferring its joint angles (blue line), even within a single trial.

In sum, these results show that the deep model is not less efficient than previous implementations and that in addition to matching their performance, it also affords self-modeling. The next simulations will show that the deep model can be additionally scaled up to account for complex kinematic chains.

Deep inference. Fig. 3 shows an evaluation of the deep kinematic model using the same robotic arm as in Fig. 2, but equipped with an increasing number of joints, all having equal length. This simulation was assessed on 1,000 trials, lasting 2,000 time steps for trial. Since we removed the angle limits, the performances are optimal for inference and near-optimal for action. Some trials fail, because the time needed to backpropagate the attractor toward the deepest levels exceeds the time limits, affecting both accuracy and mean error.

More complex control tasks. In addition to the previous simulations, the deep model can also control simpler (e.g., arm-like) and more complex (e.g., body-like) structures in a variety of tasks, which require simultaneously tracking a dynamic object (in red) while avoiding another dynamic object (in green) (Fig. 4A), making lateral movements while maintaining a vertical orientation of the last segment (Fig. 4B), performing circular movements in the Cartesian space (Fig. 4C), avoiding a dynamic object with a human-like body (Fig. 4D), reaching simultaneously multiple targets with different limbs of a human-like body (Fig. 4E), or of a tree-like body with 28 DoF and multiple ramifications (Fig. 4F); see *SI Appendix* for more information about these and various other control tasks.

Crucially, the same deep model can achieve all these (and other) tasks by simply specifying different goals, using attractive or repulsive forces, or a combination of both, without having to define ad hoc cost functions. Compared to other approaches, the deep model is therefore particularly easy to scale up to address complex kinematic structures and control problems with multiple goals.

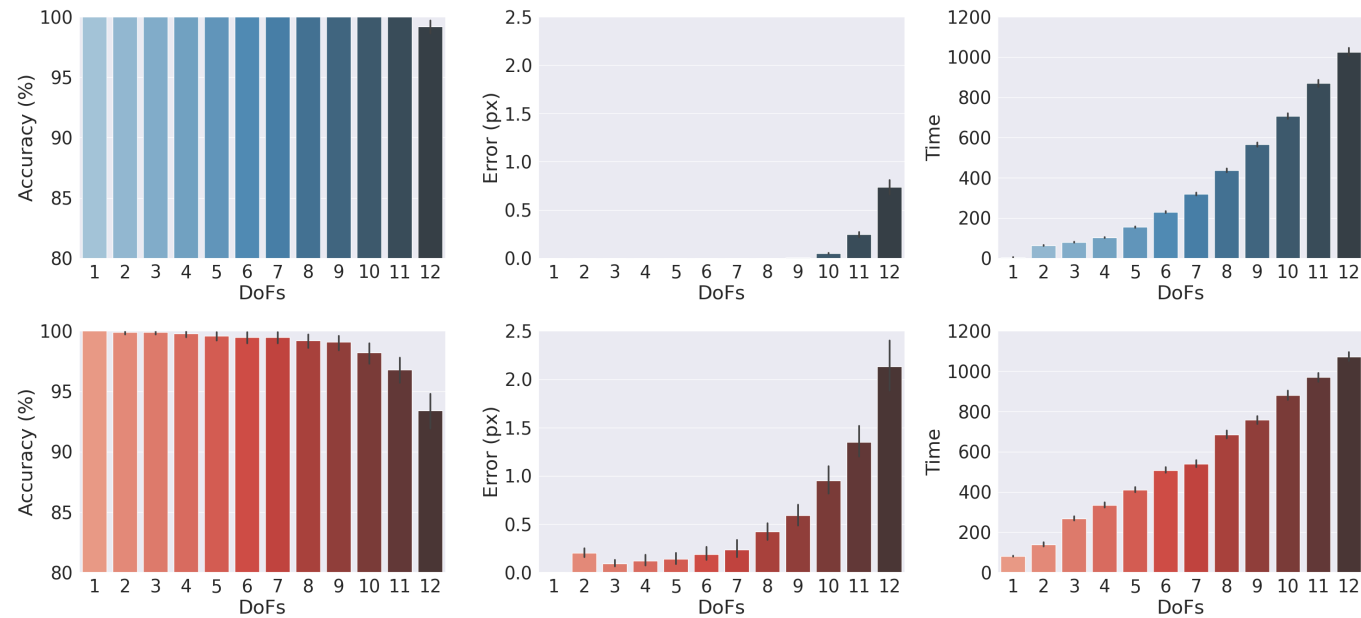


Fig. 3. Deep inference. Comparison between hierarchical models with increasing DoF (here, kinematic depth). Inference (Top) and reach (Bottom) simulations.

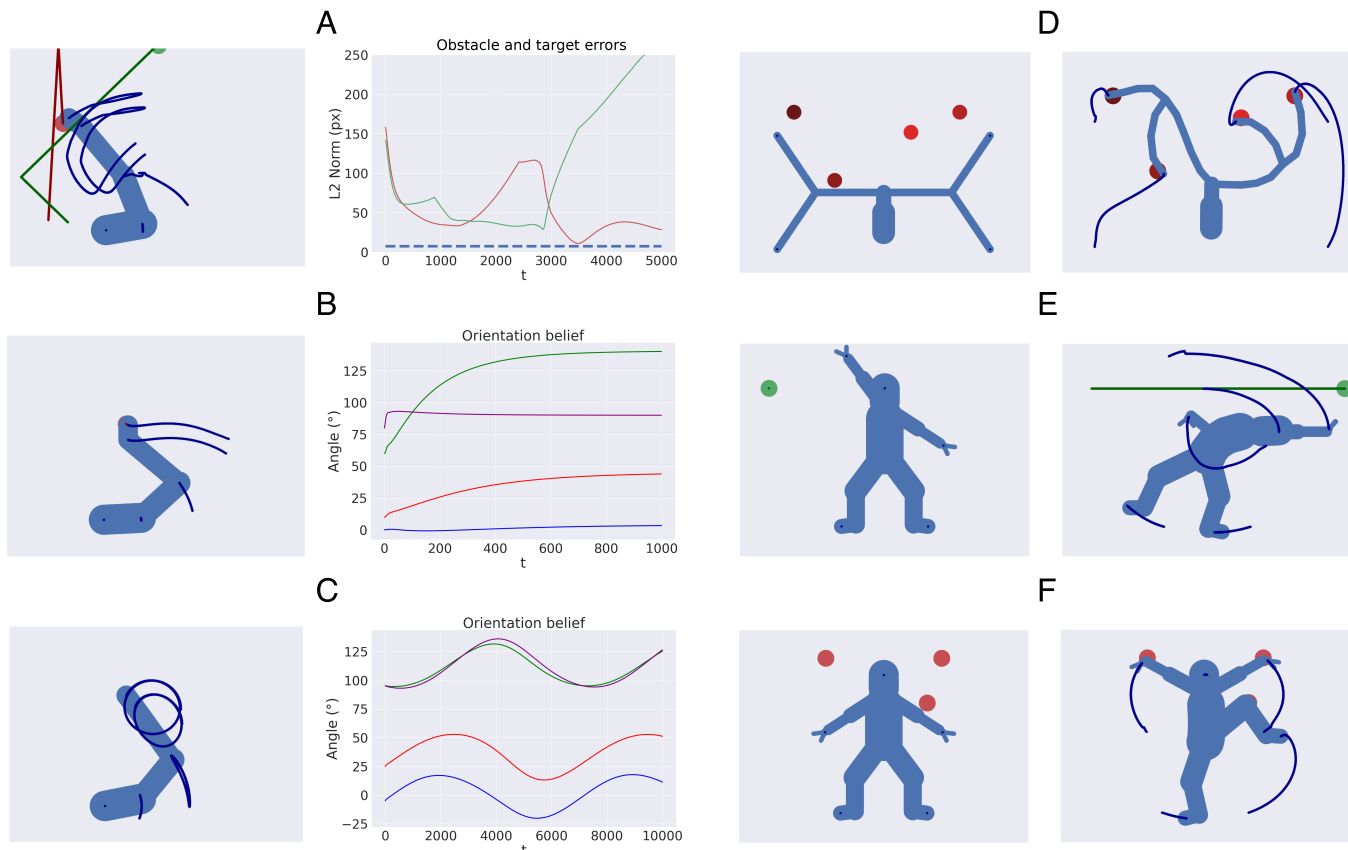


Fig. 4. Applications. Track and avoid (*A*), maintain orientation (*B*), perform circular trajectory (*C*), avoid with a full human body (*D*), reach multiple targets with a full human body (*E*), and with a more complex kinematic tree (*F*). The trajectories in the first panel represent the hand-obstacle distance (red line), the hand-target distance (green line), and the minimum distance that the target is considered to be reached (dotted blue line). Instead, the trajectories in the next two panels show the absolute orientation of every joint (in particular, the purple line is the orientation of the hand). More information about the specific tasks and other applications can be found in *SI Appendix*.

Discussion

Active inference proposes that goal-directed movements are realized by producing predictions with a generative model of the coupled agent-environment system and then minimizing the errors between predicted and current sensations. Despite its strong theoretical appeal (1), this framework has enjoyed limited applications in motor control and robotics, given the challenge of specifying appropriate generative models to map different (extrinsic and intrinsic) coordinates of movement, and to control complex kinematic structures such as the human body.

Here, we show that a generative (IE) model that maintains distinct beliefs over intrinsic and extrinsic coordinates affords effective control of goal-directed movements, because it allows defining both intrinsic and extrinsic goals as attractive (or repulsive) states and solving inverse kinematics via (active) inference, which is typically challenging in other frames like optimal control. Furthermore, we show that a deep hierarchical extension of the IE scheme drastically improves its scalability. In particular, replicating the same IE generative model for each block of the kinematic chain simplifies the computations of the direct kinematics and permits controlling complex kinematic structures that require the simultaneous coordination of multiple segments.

The proposed deep hierarchical architecture has four main advantages compared to optimal control schemes or state-of-the-art models in the active inference literature. First, it is efficient: Performing the kinematic inversion through inference drastically reduces its computational cost. Second, it is scalable:

It is possible to design generative models for sophisticated kinematic chains by simply connecting multiple IE models. Since the overall generative model always mimics the entire kinematic chain, adding or removing new segments (e.g., to model tool use) simply requires adding or removing the corresponding blocks. Third, it affords self-modeling (37) by continuously inferring the kinematic structure online and rapidly readapting to changes in limb lengths. Fourth, it affords a biologically plausible form of inference that only uses local message passing and asynchronous computations, akin to hierarchical Predictive Coding for perception (11, 34, 35, 38).

The behavior of the deep kinematic model, which replicates the same computational block across various levels, bears some analogies with deep neural networks. It is common to use the latter (e.g., Variational Autoencoders) as generative models for active inference agents (16, 30). Despite their effectiveness, the deep networks are treated as black boxes during inference: The belief over hidden states only receives a single gradient and it is unaware of the internal computations performed by the backpropagation algorithm. This has the downside that the weights of the generative model have to be learned a priori and remain constant throughout the active inference process—hence, the agent cannot adapt them when it receives novel sensory observations. Furthermore, the agent has no control over the dynamics of the generative model and cannot control the intermediate levels of the deep network toward potentially preferred states. In other words, almost all the hard work is delegated to the deep network and the only job left to the active

inference agent is inferring the highest level of the hidden states. In contrast, one appeal of Predictive Coding methods is that they can simultaneously perform hidden state inference and learning (11, 34, 35, 39). Designing a hierarchical structure that uses the same rules of prediction error minimization throughout the levels means that the agent can constantly modify its internal models to match both sensory observations and prior expectations.

In this study, we focused on the theoretical aspects of controlling a complex hierarchical structure with multiple constraints. For this reason, we used a relatively simple velocity-controlled system, without considering higher temporal orders. This implies that the dynamics functions illustrated lack some of the constraints required to smoothly actuate a real system. However, such constraints can be easily included in the active inference scheme used here, by imposing priors at specific levels of the hierarchy. We provided one example in the Results section, when we discussed how the system can incorporate specific affordances, but other useful examples can be made. Given the simple analytical form of the kinematic model, one can achieve movements with the desired smoothness by expanding the generalized state space and defining dynamics functions of increasing temporal orders, as we did for our velocity-controlled scheme. As a result, jerk minimization can be realized by maintaining an intrinsic belief with temporal orders up to the fourth and imposing a limit at the last level (19). Similarly, an attractor could be defined at the third level, setting specific torques to a joint and allowing one to simulate advanced limb dynamics (20); singularities can also be avoided by predicting their influence in advance and embedding them at the intrinsic level (12). Of note, there is a growing literature about the study of dynamics and stability properties of active inference agents (40), which have been used to design robust robotic systems operating in volatile environments (41, 42). A useful direction of research would be to combine such studies with the features of a hierarchical kinematic model that were presented here.

Advanced movements beyond reaching and avoiding tasks—such as those requiring high-level planning—may be achieved through a hybrid scheme (18), in which a discrete model plans an optimal sequence of actions that is in turn realized by a continuous model like the one exemplified in this study. In particular, the hybrid scheme allows the agent to model the environment at a more abstract level, realizing multistep reaching movements (43), object manipulation tasks (44), smooth goal-directed movements in animal behavior (45), and planning trajectories that avoid the local minima arising with artificial potential fields. We plan to simulate these and other advanced capabilities of hybrid active inference in future works. While local message passing may seem restricting, it does not hinder but rather helps achieve the high-level simultaneous coordination of all limbs. Indeed, a discrete model could still have access to and impose priors over every element of the kinematic chain, affording synchronized behavior (44). Then, the hierarchical structure of the generative model improves the movements that the agent intends to realize, by predicting the exchange of forces that will be produced locally between every couple of joints in the generative process.

Finally, although we exemplified a deep kinematic inference for the control of human body movements, the same design could be used to control other, potentially more sophisticated structures, composed of multiple ramifications. Generalizing the hierarchical connections of each level to account for arbitrary transformations between reference frames—as described in ref. 46—could be used, e.g., to estimate the depth of an object based on different

camera projections. The deep kinematic inference approach can therefore pave the way for the efficient and biologically plausible control of general actuated systems.

Materials and Methods

Hierarchical Active Inference. The core of active inference is the use of a generative model to generate predictions and minimize any prediction error resulting from discrepancies between predictions and observations. The generative model depends on three elements encoded in generalized coordinates of increasing temporal orders (e.g., position, velocity, acceleration, etc.): hidden states \tilde{x} , hidden causes \tilde{v} and sensory signals \tilde{s} . These elements are related by a nonlinear system specifying the generation of sensory signals and the evolution of latent states over time:

$$\begin{aligned}\tilde{s} &= \tilde{g}(\tilde{x}) + w_s, \\ \mathcal{D}\tilde{x} &= \tilde{f}(\tilde{x}, \tilde{v}) + w_x,\end{aligned}\quad [1]$$

where \mathcal{D} is a differential operator that shifts all the temporal orders by one, i.e., $\mathcal{D}\tilde{x} = [\tilde{x}', \tilde{x}'', \tilde{x}''', \dots]$, while w_s and w_x are noise terms assumed to be sampled from a Gaussian distribution (see refs. 11 and 47 for more details). The associated joint probability is factorized into independent distributions:

$$p(\tilde{s}, \tilde{x}, \tilde{v}) = p(\tilde{s}|\tilde{x})p(\tilde{x}|\tilde{v})p(\tilde{v}),\quad [2]$$

where each distribution is Gaussian:

$$\begin{aligned}p(\tilde{s}|\tilde{x}) &= \mathcal{N}(\tilde{g}(\tilde{x}), \tilde{\Pi}_s^{-1}), \\ p(\mathcal{D}\tilde{x}|\tilde{v}) &= \mathcal{N}(\tilde{f}(\tilde{x}, \tilde{v}), \tilde{\Pi}_x^{-1}), \\ p(\tilde{v}|\eta) &= \mathcal{N}(\eta, \tilde{\Pi}_v^{-1}),\end{aligned}\quad [3]$$

expressed in terms of precisions or inverse variances $\tilde{\Pi}_s$, $\tilde{\Pi}_x$, and $\tilde{\Pi}_v$. Following a variational inference approach (48), these distributions are inferred through approximate posteriors $q(\tilde{x})$ and $q(\tilde{v})$. Minimizing the variational free energy (VFE) \mathcal{F} , defined as the difference between the KL divergence of the (real and approximate) posteriors and the log evidence:

$$\mathcal{F} = \mathbb{E}_{q(\tilde{x})} \left[\ln \frac{q(\tilde{x})}{p(\tilde{x}, \tilde{y})} \right] = \mathbb{E}_{q(\tilde{x})} \left[\ln \frac{q(\tilde{x})}{p(\tilde{x}|\tilde{y})} \right] - \ln p(\tilde{y}),\quad [4]$$

reduces to the minimization of prediction errors. As a result, the updates of the beliefs $\tilde{\mu}$ and \tilde{v} respectively over the hidden states and hidden causes become:

$$\begin{aligned}\dot{\tilde{\mu}} - \mathcal{D}\tilde{\mu} &= -\partial_\mu \mathcal{F} = \partial \tilde{g}^T \tilde{\Pi}_s \tilde{\epsilon}_s + \partial_\mu \tilde{f}^T \tilde{\Pi}_\mu \tilde{\epsilon}_\mu - \mathcal{D}^T \tilde{\Pi}_\mu \tilde{\epsilon}_\mu, \\ \dot{\tilde{v}} - \mathcal{D}\tilde{v} &= -\partial_v \mathcal{F} = \partial_v \tilde{f}^T \tilde{\Pi}_\mu \tilde{\epsilon}_\mu - \tilde{\Pi}_v \tilde{\epsilon}_v,\end{aligned}\quad [5]$$

where $\tilde{\epsilon}_s$, $\tilde{\epsilon}_\mu$, and $\tilde{\epsilon}_v$ are respectively the prediction errors of sensory signals, dynamics, and priors:

$$\begin{aligned}\tilde{\epsilon}_s &= \tilde{s} - \tilde{g}(\tilde{\mu}), \\ \tilde{\epsilon}_\mu &= \mathcal{D}\tilde{\mu} - \tilde{f}(\tilde{\mu}, \tilde{v}), \\ \tilde{\epsilon}_v &= \tilde{v} - \eta.\end{aligned}\quad [6]$$

A simple formulation of active inference can deal with several tasks, but its main strength relies on a hierarchical structure that allows the brain to learn the inherently hierarchical relations between sensory observations and their causes (18).

This structure can be easily scaled up by linking every hidden cause with another generative model; thus, the prior becomes the prediction from the layer above, while the observation becomes the likelihood of the layer below:

$$\begin{aligned}\dot{\tilde{\mu}}^{(j)} &= \mathcal{D}\tilde{\mu}^{(j)} + \partial \tilde{g}^{(j)T} \tilde{\Pi}_v^{(j)} \tilde{\epsilon}_v^{(j)} + \partial_\mu \tilde{f}^{(j)T} \tilde{\Pi}_\mu^{(j)} \tilde{\epsilon}_\mu^{(j)} - \mathcal{D}^T \tilde{\Pi}_\mu^{(j)} \tilde{\epsilon}_\mu^{(j)}, \\ \dot{\tilde{v}}^{(j)} &= \mathcal{D}\tilde{v}^{(j)} + \partial_v \tilde{f}^{(j)T} \tilde{\Pi}_\mu^{(j)} \tilde{\epsilon}_\mu^{(j)} - \tilde{\Pi}_v^{(j-1)} \tilde{\epsilon}_v^{(j-1)},\end{aligned}\quad [7]$$

where:

$$\begin{aligned}\tilde{\epsilon}_{\mu}^{(j)} &= \mathcal{D}\tilde{\mu}_{\mu}^{(j)} - \tilde{\mathbf{f}}^{(j)}(\tilde{\mu}^{(j)}, \tilde{\mathbf{v}}^{(j)}), \\ \tilde{\epsilon}_{\nu}^{(j)} &= \tilde{\mu}_{\nu}^{(j+1)} - \tilde{\mathbf{g}}^{(j)}(\tilde{\mu}^{(j)}).\end{aligned}\quad [8]$$

On the other hand, action is realized by minimizing the proprioceptive component of the VFE with respect to the motor control signals \mathbf{a} :

$$\dot{\mathbf{a}} = -\partial_{\mathbf{a}}\mathcal{F}_p = -\partial_{\mathbf{a}}\tilde{s}_p\tilde{\Pi}_p\tilde{\epsilon}_p,\quad [9]$$

where $\partial_{\mathbf{a}}\tilde{s}_p$ is the partial derivative of proprioceptive observations with respect to the motor control signals, $\tilde{\Pi}_p$ are the precisions of proprioceptive generative models, and $\tilde{\epsilon}_p$ are the generalized proprioceptive prediction errors:

$$\tilde{\epsilon}_p = \tilde{s}_p - \tilde{\mathbf{g}}_p(\tilde{\mu}).\quad [10]$$

Kinematic Models: Belief Update. In the IE model (shown in *SI Appendix*, Fig. S1), the intrinsic belief μ_i encodes every joint angle in parallel while the extrinsic belief μ_e only encodes the Cartesian position of the end effector. Proprioceptive and visual observations are indicated by s_p and s_v . For a 2R robotic arm, the intrinsic and extrinsic beliefs are related by:

$$\begin{aligned}\mu_i &= [\theta_1 \quad \theta_2], \\ \mu_e &= [x_e \quad y_e] = \mathbf{g}_e(\mu_i), \\ &= [l_1 c_1 + l_2 c_{12} \quad l_1 s_1 + l_2 s_{12}],\end{aligned}\quad [11]$$

where \mathbf{g}_e is a generative model performing forward kinematics, and we used a compact notation to indicate the sine and cosine of the angles:

$$\begin{aligned}c_1 &= \cos(\theta_1) & c_{12} &= \cos(\theta_1 + \theta_2) = c_1 c_2 - s_1 s_2, \\ s_1 &= \sin(\theta_1) & s_{12} &= \sin(\theta_1 + \theta_2) = c_1 s_2 + s_1 c_2.\end{aligned}\quad [12]$$

The update equation for the intrinsic belief is then a combination of proprioceptive likelihood, extrinsic likelihood, and intrinsic attractor dynamics:

$$\dot{\tilde{\mu}}_i = \mathcal{D}\tilde{\mu}_i - \partial_{\mu_i}\mathcal{F} = \left[\begin{array}{c} \mu'_i + \partial \mathbf{g}_p^T \pi_p \epsilon_p + \partial \mathbf{g}_e^T \pi_e \epsilon_e + \partial \mathbf{f}_i^T \pi_{\mu_i} \epsilon_{\mu_i} \\ -\pi_{\mu_i} \epsilon_{\mu_i} \end{array} \right],\quad [13]$$

$$\dot{\tilde{\mu}}_e^{(j)} = \left[\begin{array}{c} \mu_e'^{(j)} - \pi_e^{(j)} \epsilon_e^{(j)} + \sum_m \partial_{\mu_e} \mathbf{g}_e^T \pi_e^{(j+1,m)} \epsilon_e^{(j+1,m)} + \partial \mathbf{g}_v^T \pi_v^{(j)} \epsilon_v^{(j)} + \partial \mathbf{f}_e^{(j)^T} \pi_{\mu_e}^{(j)} \epsilon_{\mu_e}^{(j)} \\ -\pi_{\mu_e}^{(j)} \epsilon_{\mu_e}^{(j)} \end{array} \right].\quad [22]$$

where \mathbf{g}_p is the proprioceptive likelihood function, while ϵ_p and ϵ_e are the proprioceptive and kinematic prediction errors:

$$\begin{aligned}\epsilon_p &= s_p - \mathbf{g}_p(\mu_i), \\ \epsilon_e &= \mu_e - \mathbf{g}_e(\mu_i).\end{aligned}\quad [14]$$

The form of the dynamics function \mathbf{f}_i is explained in the following sections. Note that, although the intrinsic belief includes components up to the first order, the proprioceptive generative model only produces prediction over the 0th order (i.e., position). The kinematic inversion is performed through the gradient $\partial \mathbf{g}_e$:

$$\partial \mathbf{g}_e = \begin{bmatrix} -l_1 s_1 - l_2 s_{12} \\ l_1 c_1 + l_2 c_{12} \end{bmatrix}.\quad [15]$$

Similarly, the update for the extrinsic belief is a combination of intrinsic prior, visual likelihood, and extrinsic attractor dynamics:

$$\dot{\tilde{\mu}}_e = \mathcal{D}\tilde{\mu}_e - \partial_{\mu_e}\mathcal{F} = \left[\begin{array}{c} \mu'_e - \pi_e \epsilon_e + \partial \mathbf{g}_v^T \pi_v \epsilon_v + \partial \mathbf{f}_e^T \pi_{\mu_e} \epsilon_{\mu_e} \\ -\pi_{\mu_e} \epsilon_{\mu_e} \end{array} \right],\quad [16]$$

where \mathbf{g}_v is the visual likelihood function, and ϵ_v is the visual prediction error:

$$\epsilon_v = s_v - \mathbf{g}_v(\mu_e).\quad [17]$$

As regards the motor control signals, they are computed as in Eq. 9, but only by minimizing the 0th-order proprioceptive prediction error ϵ_p :

$$\dot{\mathbf{a}} = -\Delta_t \pi_p \epsilon_p,\quad [18]$$

where we approximated the gradient $\partial_{\mathbf{a}} s_p$ by a time constant Δ_t (49), since the agent is velocity-controlled.

Concerning the deep kinematic model, if we consider a simple 2D arm, each block is composed of an intrinsic belief over pairs of joint angles and segment lengths $\mu_i^{(j)} = [\theta^{(j)}, l^{(j)}]$ and an extrinsic belief over the position of the segment's extremity and its absolute orientation $\mu_e^{(j)} = [x^{(j)}, y^{(j)}, \phi^{(j)}]$. The resulting kinematic generative model is:

$$\mu_e^{(j)} = \mathbf{g}_e(\mu_i^{(j)}, \mu_e^{(j-1)}) = \begin{bmatrix} x^{(j-1)} + l^{(j)} c_{\theta, \phi}^{(j)} \\ y^{(j-1)} + l^{(j)} s_{\theta, \phi}^{(j)} \\ \phi^{(j-1)} + \theta^{(j)} \end{bmatrix}.\quad [19]$$

The update of the intrinsic belief (Eq. 20) is equivalent to the IE model.

$$\dot{\tilde{\mu}}_i^{(j)} = \left[\begin{array}{c} \mu_i'^{(j)} + \partial \mathbf{g}_p^T \pi_p^{(j)} \epsilon_p^{(j)} + \partial \mu_i \mathbf{g}_e^T \pi_e^{(j+1)} \epsilon_e^{(j+1)} + \partial \mathbf{f}_i^{(j)^T} \pi_{\mu_i}^{(j)} \epsilon_{\mu_i}^{(j)} \\ -\pi_{\mu_i}^{(j)} \epsilon_{\mu_i}^{(j)} \end{array} \right].\quad [20]$$

However, $\epsilon_p^{(j)}$ now only encodes the prediction error of a single joint. Further, the gradient of the kinematic generative model with respect to the intrinsic belief is simpler, since it only depends on the intrinsic components of that level:

$$\frac{\partial \mathbf{g}_e}{\partial \mu_i^{(j)}} = \begin{bmatrix} \partial_{\theta} \mathbf{g}_e \\ \partial_{\mathbf{g}_e} \end{bmatrix} = \begin{bmatrix} -l^{(j)} s_{\theta, \phi}^{(j)} & l^{(j)} c_{\theta, \phi}^{(j)} & 1 \\ c_{\theta, \phi}^{(j)} & s_{\theta, \phi}^{(j)} & 0 \end{bmatrix}.\quad [21]$$

Note that the second row of the gradient in Eq. 21 allows inferring and learning segment lengths.

The update of the extrinsic belief (Eq. 22) still includes every component of the IE model (although separately for each joint), but with the addition of the extrinsic likelihood from the next layer $\partial_{\mathbf{g}_e}$, which in this case is the sum of all the segments it is attached to.

The gradient of this new term connects every layer in the hierarchy since intrinsic beliefs communicate with their extrinsic predictions by:

$$\frac{\partial \mathbf{g}_e}{\partial \mu_e^{(j)}} = \begin{bmatrix} \partial_x \mathbf{g}_e \\ \partial_y \mathbf{g}_e \\ \partial_{\phi} \mathbf{g}_e \end{bmatrix} = \begin{bmatrix} 1 & 0 & 0 \\ 0 & 1 & 0 \\ -l^{(j)} s_{\theta, \phi}^{(j)} & l^{(j)} c_{\theta, \phi}^{(j)} & 1 \end{bmatrix}.\quad [23]$$

Overall, the main differences between the IE model and the basic block of the hierarchical model are i) in the former, a single level encodes J joint angles in parallel (where J is the number of joint angles), while the latter is composed of J levels each encoding a single joint angle; ii) in the basic block of the hierarchical model, there is an additional connection from the extrinsic belief μ_e of level $j-1$ to the extrinsic belief of level j .

Ramifications. If we consider a ramification with M extrinsic outputs $\mu_e^{(j+1,m)} = \mathbf{g}_e(\mu_i^{(j+1)}, \mu_e^{(j)})$, the update equation for the parent node $\mu_e^{(j)}$ is proportional to:

$$\dot{\mu}_e^{(j)} \propto \sum_m \partial_{\mu_e} \mathbf{g}_e^T \pi_e^{(j+1,m)} \epsilon_e^{(j+1,m)},\quad [24]$$

where $\epsilon_e^{(j+1,m)}$ is the extrinsic prediction error of block $(j+1, m)$ and $\pi_e^{(j+1,m)}$ is the corresponding precision. The latter thus weighs the contribution for each branch of the level.

Defining Attractive Goals and Repulsive Forces. Goals can be flexibly formulated at both intrinsic and extrinsic levels through an intention function $i(\mu)$ that linearly combines the current belief with biases h^* to define the desired future state μ^* (16):

$$\mu^* = i(\mu) = H\mu + h^*. \quad [25]$$

In brief, the matrix H performs a transformation of the current belief: Manipulating and combining only specific components affords a dynamic behavior (e.g., reaching a moving target), while using an identity transformation for the other components lets them free to change since their prediction error would be zero. Instead, the vector h^* is used to impose a static configuration.

This function could specify, for example, the desired angle θ^* of a joint (i.e., an intrinsic goal), the desired absolute position (x^*, y^*) or the orientation ϕ^* of a limb (i.e., extrinsic goals):

$$\begin{aligned} i_\theta^{(j)}(\mu_i^{(j)}) &= [\theta^* \quad l^{(j)}], \\ i_p^{(j)}(\mu_e^{(j)}) &= [x^* \quad y^* \quad \phi^{(j)}], \\ i_\phi^{(j)}(\mu_e^{(j)}) &= [x^{(j)} \quad y^{(j)} \quad \phi^*]. \end{aligned} \quad [26]$$

All these functions may be realized by a linear combination of the quantities defined in Eq. 25. Imposing a desired angle θ^* would be achieved by:

$$H = \begin{bmatrix} 0 & 0 \\ 0 & 1 \end{bmatrix} \quad h^* = [\theta^* \quad 0]. \quad [27]$$

Beyond static reaching, it is possible to realize a dynamic behavior through the matrix H , e.g., by imposing that the x coordinate of the end effector will match the y coordinate:

$$H = \begin{bmatrix} 0 & 1 & 0 \\ 0 & 1 & 0 \\ 0 & 0 & 1 \end{bmatrix} \quad h^* = [0 \quad 0 \quad 0]. \quad [28]$$

The same mechanism may be used to track a moving target, which is constantly inferred through visual observations, as done in ref. 16.

Attractors are then embedded into the dynamics function, which linearly minimizes the distance between the desired and current states, i.e., $f_a(\mu) = k_a \mathbf{e}_a$, where k_a is an attractive gain and $\mathbf{e}_a = \mu^* - \mu$. For simplicity, we did not consider the hidden causes of Eq. 1, thus the dynamics function only depends on the hidden states.

In turn, following the artificial potential fields theory, repulsive forces can be defined as

$$f_r(\mu) = \begin{cases} k_r \cdot (1/\gamma - 1/\|\mathbf{e}_r\|) \cdot \mathbf{e}_r / \|\mathbf{e}_r\|^3, & \text{if } \|\mathbf{e}_r\| \leq \gamma \\ 0, & \text{otherwise,} \end{cases} \quad [29]$$

where k_r is a repulsive gain, γ is the range of influence of the repulsive force, $\mathbf{e}_r = \mu^\# - \mu$ is the difference between a repulsive state $\mu^\#$ and the belief, and $\mu^\#$ is defined flexibly in the same way as the goal state μ^* . At this point, one can linearly combine attractive and repulsive forces into the dynamics function of a single level in order to achieve a complex behavior—e.g., reaching a target with the end effector while avoiding an obstacle:

$$\mu' = \sum_n f_n(\mu). \quad [30]$$

Note that these dynamics functions are always optimistically biased toward the goal states. Although not problematic in our case, a more advanced controller such as the one proposed in ref. 50 would provide unbiased state estimates which may be critical for realistic settings (e.g., for handling collisions) and with adaptable precisions.

Assessment Metrics. The three metrics used to evaluate perceptual inference are i) perception accuracy: success in finding a joint configuration corresponding to the true target location within 8 pixels; ii) perception error: L^2 distance between the true and estimated target positions at the end of the trial; iii) perception time: number of time steps needed to successfully estimate the target position.

The three metrics used to evaluate reaching are iv) reach accuracy: success in approaching the target within 8 pixels; v) reach error: L^2 end effector-target distance at the end of the trial; vi) reach time: number of time steps needed for the end effector to reach the target in successful trials. Note that the reaching task is more challenging than the inference task, since it requires inferring the final arm configuration based on information about only the position of the last segment.

Data, Materials, and Software Availability. Method data have been deposited in GitHub (<https://github.com/priorelli/deep-kinematic-inference>) (51).

ACKNOWLEDGMENTS. This research received funding from the European Union's Horizon H2020-EIC-FETPROACT-2019 Programme for Research and Innovation under Grant Agreement 951910 to I.P.S., the European Union's Horizon 2020 Framework Programme for Research and Innovation under Grant Agreement 945539 to G.P., the European Research Council under the Grant Agreement 820213 to G.P., and the Italian Ministry for Research MIUR, under Grant Agreements PRIN 2017KZNZLN to I.P.S. and PE0000013-FAIR and IR0000011-EBRAINS-Italy to G.P. The GEFORCE Quadro RTX6000 and Titan GPU cards used for this research were donated by the NVIDIA Corporation. The funders had no role in study design, data collection and analysis, decision to publish, or preparation of the manuscript.

1. M. Floegl, J. Kasper, P. Perrier, C. A. Kell, How the conception of control influences our understanding of actions. *Nat. Rev. Neurosci.* **24**, 313–329 (2023).
2. E. Todorov, Optimality principles in sensorimotor control. *Nat. Neurosci.* **7**, 907–915 (2004).
3. J. Diedrichsen, R. Shadmehr, R. B. Ivry, The coordination of movement: Optimal feedback control and beyond. *Trends Cogn. Sci.* **14**, 31–39 (2010).
4. R. Shadmehr, M. A. Smith, J. W. Krakauer, Error correction, sensory prediction, and adaptation in motor control. *Annu. Rev. Neurosci.* **33**, 89–108 (2010).
5. D. McNamee, D. M. Wolpert, Internal models in biological control. *Annu. Rev. Control, Rob., Auton. Syst.* **2**, 339–364 (2019).
6. R. F. Stengel, *Optimal Control and Estimation* (Courier Corporation, 1994).
7. K. Friston, What is optimal about motor control? *Neuron* **72**, 488–498 (2011).
8. D. W. Franklin, D. M. Wolpert, Computational mechanisms of sensorimotor control. *Neuron* **72**, 425–442 (2011).
9. M. M. Hayhoe, Vision and action. *Annu. Rev. Vis. Sci.* **3**, 389–413 (2017).
10. K. J. Friston, J. Daunizeau, J. Kilner, S. J. Kiebel, Action and behavior: A free-energy formulation. *Biol. Cybern.* **102**, 227–260 (2010).
11. T. Parr, G. Pezzulo, K. J. Friston, *Active Inference: The Free Energy Principle in Mind, Brain, and Behavior* (MIT Press, 2022).
12. L. Pio-Lopez, A. Nizard, K. Friston, G. Pezzulo, Active inference and robot control: A case study. *J. R. Soc. Interface* **13**, 20160616 (2016).
13. R. A. Adams, S. Shipp, K. J. Friston, Predictions not commands: Active inference in the motor system. *Brain Struct. Funct.* **218**, 611–643 (2013).
14. M. Baltieri, C. L. Buckley, "Active inference: Computational models of motor control without efference copy" in *Proceedings of the 2019 Conference on Cognitive Computational Neuroscience* (ACM, New York, NY, 2019).
15. P. Lanillos, G. Cheng, "Adaptive robot body learning and estimation through predictive coding" in *IEEE International Conference on Intelligent Robots and Systems* (2018), pp. 4083–4090.
16. M. Priorelli, I. P. Stoianov, Flexible intentions: An active inference theory. *Front. Comput. Neurosci.* **17**, 1–41 (2023).
17. H. Brown, K. Friston, S. Bestmann, Active inference, attention, and motor preparation. *Front. Psychol.* **2**, 1–10 (2011).
18. K. Friston, T. Parr, B. de Vries, The graphical brain: Belief propagation and active inference. *Netw. Neurosci.* **1**, 222–241 (2018).
19. M. Baioumy, P. Duckworth, B. Lacerda, N. Hawes, "Active inference for integrated state-estimation, control, and learning" in *2021 IEEE International Conference on Robotics and Automation (ICRA)* (2021), pp. 4665–4671.
20. C. Meo, G. Franzese, C. Pezzato, M. Spahn, P. Lanillos, Adaptation through prediction: Multisensory active inference torque control. *IEEE Trans. Cogn. Dev. Syst.* **15**, 32–41 (2023).
21. A. Ciria, G. Schillaci, G. Pezzulo, V. V. Hafner, B. Lara, Predictive processing in cognitive robotics: A review. *Neural Comput.* **33**, 1402–1432 (2021).

22. A. Maselli, P. Lanillos, G. Pezzulo, Active inference unifies intentional and conflict-resolution imperatives of motor control. *PLoS Comput. Biol.* **18**, e1010095 (2022).
23. F. Mannella, F. Maggiore, M. Baltieri, G. Pezzulo, Active inference through whiskers. *Neural Netw.* **144**, 428–437 (2021).
24. T. Taniguchi et al., World models and predictive coding for cognitive and developmental robotics: Frontiers and challenges. *Adv. Rob.* **37**, 780–806 (2023).
25. A. Ahmadi, J. Tani, A novel predictive-coding-inspired variational RNN model for online prediction and recognition. *Neural Comput.* **31**, 2025–2074 (2019).
26. C. Pezzato, R. Ferrari, C. H. Corbato, A novel adaptive controller for robot manipulators based on active inference. *IEEE Rob. Autom. Lett.* **5**, 2973–2980 (2020).
27. P. Mazzaglia, T. Verbelen, O. Catal, B. Dhoedt, The free energy principle for perception and action: A deep learning perspective. *Entropy* **24**, 301 (2022).
28. O. Catal, T. Verbelen, T. Van de Maele, B. Dhoedt, A. Safron, Robot navigation as hierarchical active inference. *Neural Netw.* **142**, 192–204 (2021).
29. T. Matsumoto, J. Tani, Goal-directed planning for habituated agents by active inference using a variational recurrent neural network. *Entropy* **22**, 564 (2020).
30. C. Sancaktar, M. A. J. van Gerven, P. Lanillos, “End-to-end pixel-based deep active inference for body perception and action” in *IEEE International Conference on Development and Learning and Epigenetic Robotics* (2020), pp. 1–8.
31. K. J. Friston, J. Mattout, J. Kilner, Action understanding and active inference. *Biol. Cybern.* **104**, 137–60 (2011).
32. G. Oliver, P. Lanillos, G. Cheng, An empirical study of active inference on a humanoid robot. *IEEE Trans. Cogn. Dev. Syst.* **14**, 462–471 (2021).
33. R. Bogacz, A tutorial on the free-energy framework for modelling perception and learning. *J. Math. Psychol.* **76**, 198–211 (2017).
34. K. Friston, A theory of cortical responses. *Philos. Trans. R. Soc. B: Biol. Sci.* **360**, 815–836 (2005).
35. R. P. N. Rao, D. H. Ballard, Predictive coding in the visual cortex: A functional interpretation of some extra-classical receptive-field effects. *Nat. Neurosci.* **2**, 79–87 (1999).
36. M. Priorelli, I. P. Stoianov, “Intention modulation for multi-step tasks in continuous time active inference” in *3rd International Workshop on Active Inference (IWAI 2022)* (Grenoble, 2022).
37. J. Bongard, V. Zykov, H. Lipson, Resilient machines through continuous self-modeling. *Science* **314**, 1118–1121 (2006).
38. C. L. Buckley, C. S. Kim, S. McGregor, A. K. Seth, The free energy principle for action and perception: A mathematical review. *J. Math. Psychol.* **81**, 55–79 (2017).
39. A. Ororbia, D. Kifer, The neural coding framework for learning generative models. *Nat. Commun.* **13**, 2064 (2022).
40. A. A. Meera, M. Wisse, Dynamic expectation maximization algorithm for estimation of linear systems with colored noise. *Entropy* **23**, 1306 (2021).
41. A. A. Meera, P. Lanillos, Adaptive noise covariance estimation under colored noise using dynamic expectation maximization. arXiv [Preprint] (2023). <https://doi.org/10.48550/arXiv.2308.07797> (Accessed 20 August 2023).
42. F. Bos, A. A. Meera, D. Benders, M. Wisse, “Free energy principle for state and input estimation of a quadcopter flying in wind” in *Proceedings—IEEE International Conference on Robotics and Automation* (2022), pp. 5389–5395.
43. T. Parr, J. Limanowski, V. Rawji, K. Friston, The computational neurology of movement under active inference. *Brain* **144**, 1799–1818 (2021).
44. M. Priorelli, I. P. Stoianov, Slow but flexible or fast but rigid? Discrete and continuous processes compared. bioRxiv [Preprint] (2023). <https://doi.org/10.1101/2023.08.20.554008> (Accessed 21 August 2023).
45. V. H. Sridhar et al., The geometry of decision-making in individuals and collectives. *Proc. Natl. Acad. Sci. U.S.A.* **118**, e2102157118 (2021).
46. M. Priorelli, G. Pezzulo, I. P. Stoianov, Active vision in binocular depth estimation: A top-down perspective. *Biomimetics* **8**, 445 (2023).
47. K. Friston et al., The free energy principle made simpler but not too simple. *Phys. Rep.* **1024**, 1–29 (2022).
48. K. Friston, J. Mattout, N. Trujillo-Barreto, J. Ashburner, W. Penny, Variational free energy and the Laplace approximation. *Neuroimage* **34**, 220–234 (2007).
49. G. Oliver, P. Lanillos, G. Cheng, Active inference body perception and action for humanoid robots. arXiv [Preprint] (2019). <https://doi.org/10.48550/arXiv.1906.03022> (Accessed 1 May 2023).
50. M. Baioumy, C. Pezzato, R. Ferrari, N. Hawes, “Unbiased active inference for classical control” in *2022 IEEE/RSJ International Conference on Intel Robots and Systems (IROS)* (2022), pp. 12787–12794.
51. M. Priorelli, Method data of: Deep kinematic inference affords efficient and scalable control of bodily movements. Github. <https://github.com/priorelli/deep-kinematic-inference>. Deposited 1 November 2023.